Prostaglandin E_2 Induces Breast Cancer–Related Aromatase Promoters via Activation of p38 and c-Jun NH_2-Terminal Kinase in Adipose Fibroblasts

Dong Chen, Scott Reierstad, Zhihong Lin, Meiling Lu, Chris Brooks, Newton Li, Joy Innes, and Serdar E. Bulun

Division of Reproductive Biology Research, Department of Obstetrics and Gynecology, Northwestern University, Chicago, Illinois

Abstract

Aromatase is the key enzyme for estrogen biosynthesis. A distal promoter, PI.4, maintains baseline levels of aromatase in normal breast adipose tissue. In contrast, malignant breast epithelial cells secrete prostaglandin E_2 (PGE_2), which stimulates aromatase expression via proximal promoters PI.3/PII in a cyclic AMP (cAMP)– and protein kinase C (PKC)–dependent manner in adjacent breast adipose fibroblasts (BAF), leading to increased local concentrations of estrogen. Although an effective treatment for breast cancer, aromatase inhibitors indiscriminately abolish estrogen synthesis in all tissues, causing major side effects. To identify drug targets to selectively block aromatase and estrogen production in breast cancer, we investigated PGE_2-stimulated signaling pathways essential for aromatase induction downstream of cAMP and PKC in human BAFs. Here, we show that PGE_2 or its surrogate hormonal mixture dibutyryl cAMP (Bt_2cAMP) + phorbol diacetate (PDA) stimulated the p38, c-jun NH_2-terminal kinase (JNK)-1, and extracellular signal–regulated kinase (ERK) mitogen-activated protein kinase pathways. Inhibition or small interfering RNA–mediated knockdown of p38 or JNK1, but not ERK, inhibited PGE_2- or Bt_2cAMP + PDA–induced aromatase activity and expression via PI.3/PII. Conversely, overexpression of wild-type p38α or JNK1 enhanced PGE_2-stimulated aromatase expression via PII. PGE_2 or Bt_2cAMP + PDA stimulated c-Jun and activating transcription factor-2 (ATF2) phosphorylation and binding to the PI.3/PII region. Specific activation of protein kinase A (PKA) or EPAC with cAMP analogues stimulated p38 and JNK1; however, only PKA-activating cAMP analogues induced aromatase expression. The PKC activator PDA effectively stimulated p38 and JNK1 phosphorylation but not aromatase expression. Taken together, PGE_2 activation of p38 and JNK1 via PKA and PKC is necessary for aromatase induction in BAFs, and p38 and JNK1 are potential new drug targets for tissue-specific ablation of aromatase expression in breast cancer. [Cancer Res 2007;67(18):8914–22]

Introduction

Aromatase catalyzes the conversion of C_{19} steroids to estrogens in a number of human cells and tissues, including ovarian granulosa cells and skin and adipose fibroblasts, hypothalamic neurons, bone, and the placental syncytiotrophoblast (1). A single gene, *CYP19*, encodes aromatase. Aromatase expression in adipose tissue is restricted to undifferentiated fibroblasts and not detected in significant quantities in fully differentiated, lipid-filled adipocytes (1). Disproportionately high aromatase expression and activity in undifferentiated breast adipose fibroblasts (BAF) adjacent to malignant epithelial cells likely contributes to breast cancer development and progression (2, 3). Moreover, malignant epithelial cells secrete tumor necrosis factor (TNF) and interleukin (IL)-11, which maintain BAFs in an undifferentiated state (4). These fibroblasts are compacted around malignant cells and provide structural support for the tumor (4). This relationship, in which BAFs provide functional support for cancer growth, is supported by the observation that the breast quadrant bearing a malignant tumor consistently displays the highest levels of aromatase activity (2).

Expression of aromatase is controlled by several distinct and partially tissue-specific promoters (5). The coding region of aromatase transcripts and the translated protein, however, are identical in all tissues where aromatase is expressed (6, 7). In adipose tissue, three promoters are used. In disease-free breast adipose tissue, aromatase is usually expressed at low levels via distal promoter I.4, whereas in breast adipose tissue bearing a tumor, aromatase expression is activated via two proximally located promoters, I.3 and II (1). Currently, competitive or suicidal aromatase inhibitors are the most effective endocrine treatment of breast cancer (1, 8). However, these agents lead to indiscriminate reduction of aromatase expression throughout the body, resulting in severe estrogen deprivation and major side effects, including hot flashes, bone loss, increased fracture rates, and abnormal lipid metabolism (9). That activation of promoters I.3 and II leads to up-regulation of aromatase expression in breast cancer provides an opportunity to develop new breast cancer treatments that specifically target pathways leading to PI.3/PII activation.

To this end, it is important to identify the mechanisms by which aromatase PI.3/PII are activated in breast cancer adipose fibroblasts. PI.3 and PII are located within 215 bp from each other and are coordinately regulated by distinct hormonal stimuli (1). Zhao et al. (10) found that prostaglandin E_2 (PGE_2) was a potent stimulator of aromatase expression via PI.3/PII, and several lines of evidence suggest that PGE_2 is involved in breast cancer development and progression (11, 12). Breast tumor epithelial cells secrete large amounts of PGE_2 as a result of up-regulated cyclooxygenase-2 expression (13), and high levels of PGE_2 production are also

Note: Supplementary data for this article are available at Cancer Research Online (http://cancerres.aacrjournals.org/).

Requests for reprints: Dong Chen, Division of Reproductive Biology Research, Department of Obstetrics and Gynecology, Northwestern University, 303 East Superior Street, Chicago, IL 60611. Phone: 312-503-3761; Fax: 312-503-0095; E-mail: dongchen@northwestern.edu.

doi:10.1158/0008-5472.CAN-06-4751

observed in other cell types, including fibroblasts, macrophages, and lymphocytes, in breast tumor (11, 12).

In human BAFs, PGE_2 regulates aromatase expression through the EP_1, EP_2, and EP_3 prostanoid receptor subtypes (10, 14). PGE_2 binding to EP_1 leads to activation of protein kinase C (PKC). EP_2 stimulates, whereas EP_3 inhibits, the adenylate cyclase-protein kinase A (PKA) signaling pathway (15). Both PKA- and PKC-dependent signaling events are required for maximal PGE_2-induced aromatase expression (6, 16). PKC-dependent signaling synergistically enhances PKA-dependent stimulation of aromatase PI.3/PII (17). Thus, cyclic AMP (cAMP) analogues that activate PKA strongly induce aromatase activity in BAFs, and this induction is potentiated by phorbol esters that activate PKC (16). Several studies have used a surrogate hormonal mixture of dibutyryl cAMP (Bt_2cAMP) plus phorbol diacetate (PDA) to mimic PGE_2-stimulated intracellular signaling and aromatase expression (6, 16, 17).

Signaling events downstream of PKA and PKC leading to aromatase expression are unknown. The p38 mitogen-activated protein kinase (MAPK) has been implicated in follicle-stimulating hormone–stimulated aromatase expression in granulosa cells (18), and activating transcription factor 2 (ATF2), which is an *in vivo* substrate of p38 (19), was shown to bind to aromatase PI.3/PII in response to treatment of malignant epithelial cell–conditioned medium in BAFs (19, 20). p38, the c-jun NH_2-terminal kinase (JNK), and extracellular signal–regulated kinase (ERK) MAPK are activated by environmental stress (e.g., UV and osmotic shock), proinflammatory cytokines (e.g., TNF and IL-1), growth factors (e.g., epidermal growth factor), and tumor promoters (e.g., phorbol esters), and have important roles in regulation of gene expression, cell proliferation, and apoptosis (21–25). Four isoforms of p38 (α, β, γ, and δ) have been identified (25). p38α and p38β are sensitive to inhibitors such as SB202190 (25). There are three major JNK isoforms: JNK1, JNK2, and JNK3 (22). Relevant to our study is JNK1, which has four splice variants: the longer JNK1α2 and JNK1β2 and the shorter JNK1α1 and JNK1β1 (22). Stimulation of p38, JNK, and ERK requires dual phosphorylation of threonine and tyrosine residues, which occurs as a consequence of sequential activation of pathway-specific sets of MAP3Ks and MAP2Ks (22, 23).

In addition to PKA, EPAC1 and EPAC2 (exchange proteins directly activated by cAMP) have been identified as novel effectors for cAMP (26). EPACs are guanine nucleotide exchange factors for the small G protein Rap1 (26). cAMP-dependent and phorbol ester/PKC–dependent activations of p38, JNK, and ERK have been reported (18, 21, 27–31). For example, β-adrenergic stimulation of p38 is blocked by a PKA inhibitor in brown adipocytes. Pituitary adenylate cyclase–activating polypeptide stimulates p38 in neuronal cells via cAMP/EPAC (32). cAMP activates JNK in certain cell types, and the Ras exchange motif domain of EPAC has been found to be sufficient to stimulate JNK (31, 33). The mechanisms whereby cAMP and PKA stimulate the p38 and JNK cascades, however, remain poorly understood. Both PKA and EPAC can also mediate cAMP activation of ERK (30, 34). PKA activation of ERK requires C3G, another guanine nucleotide exchange factor for Rap1, to bring Rap1 to the plasma membrane and stimulate the Raf-MAPK/ERK kinase (MEK)-ERK kinase cascade (30), whereas EPAC directly activates the Rap1-Raf-B-MEK-ERK cascade (34). PKC-dependent activation of p38, JNK, and ERK involves Ras (24, 25), and the adapter protein receptor for activated C-kinase (RACK1) augments PKC activation of JNK (35).

In this study, we examined activation of p38, JNK, and ERK by PGE_2 or Bt_2cAMP + PDA in BAFs and determined the roles of these MAPKs in induction of aromatase expression and activity. We report here that PGE_2 or Bt_2cAMP + PDA stimulates all three members of the MAPK family, and that activation of p38 and JNK1 is necessary for PGE_2 or Bt_2cAMP + PDA stimulation of aromatase expression via promoters I.3/II.

Materials and Methods

Materials. Bt_2cAMP and PDA were purchased from Sigma. PKA-specific 6-MB-cAMP and EPAC-specific 8-pCPT-2′-*O*-Me-cAMP were purchased from Biolog-Life Science Institute. PGE_2 was purchased from Cayman Chemicals. Antibodies against phospho-MKK4, MKK4, phospho-p38, p38, phospho-ATF2 (Thr^{71}), ATF2, phospho-JNK, JNK, phospho-c-Jun (Ser^{63} or Ser^{73}), c-Jun, phospho-ERK, and ERK were purchased from Cell Signaling Technology, Inc. The p38 inhibitor SB202190, JNK inhibitor AS601245, and MEK inhibitor PD98059 were purchased from EMD Biosciences. The LacZ adenovirus was a gift from Dr. Ronald Kahn (Joslin Diabetes Center and Harvard Medical School, Boston, MA). The p38α and JNK1 adenoviruses were purchased from Seven Hills Bioreagents.

Cell culture. Human adipose tissue samples were obtained at the time of surgery from women undergoing reduction mammoplasty following a protocol approved by the Institutional Review Board for Human Research of Northwestern University (Chicago, IL). Isolation and culturing of primary human BAFs were done as previously described (20). Cells were grown to confluence and placed in serum-free medium for 16 h before treatment.

Adenoviral infection. Adenoviruses were amplified in HEK293 cells and purified by CsCl gradient ultracentrifugation. They were applied at a multiplicity of infection (MOI) of 20 to confluent BAFs and allowed to express for 36 h before BAFs underwent serum deprivation and treatment.

Hormonal treatments. Following serum starvation, BAFs were incubated in serum-free DMEM/F-12 medium containing 1 μmol/L PGE_2 or 0.5 mmol/L Bt_2cAMP and/or 100 nmol/L PDA for various periods of time as indicated in the figure legends. When kinase inhibitors were applied, cells were preincubated for 1 h with the inhibitors or with DMSO (vehicle control) of the same volume.

Cell extract preparation and immunoblotting. Cell extracts were prepared as previously described (36). The Bradford assay was used to quantify protein concentrations (Bio-Rad). Immunoblotting was done with primary antibodies, as indicated, followed by a horseradish peroxidase–conjugated secondary antibody (Pierce). All Western blots were developed with enhanced chemiluminescence reagents (Pierce).

TaqMan-based real-time PCR for total aromatase mRNA and promoter-specific mRNA. Total RNA was isolated from cells with Trireagent (Sigma) and reverse transcribed with the Superscript III cDNA synthesis system (Invitrogen). For total aromatase mRNA (coding region-specific) real-time PCR, the forward and reverse primers were 5′-CACATCCTCAATACCAGGTCC-3′ and 5′-CAGAGATCCAGACTCGCATG-3′, and the fluorescence-labeled probe was 5′-CCCTCATCTCCCACGGCA-GATTCC-3′. For glyceraldehyde-3-phosphate dehydrogenase (GAPDH) mRNA (control), the forward and reverse primers were 5′-GAAGGTGA-AGGTCGGAGTC-3′ and 5′-GAAGATGGTGATGGGATTTC-3′, and the probe was 5′-CAAGCTTCCCGTTCTCAGCC-3′. For aromatase PII– and PI.3–derived mRNA real-time PCR, single-stranded cDNA was first amplified by two cycles of PCR with the PII or PI.3 primer sets, composed of their respective forward primers 5′-GCAACAGGAGCTATAGATGAAC-3′ (PII) and 5′-GTCTTGCCTAAATGTCTGATCAC-3′ (PI.3) and the common reverse primer 5′-CAGAGATCCAGACTCGCATG-3′. The single-stranded cDNA template and double-stranded DNA product were purified by the high pure PCR product purification kit (Roche). One aliquot of the purified DNA sample was treated with *Exo*I to remove the single-stranded cDNA template, and the amount of the remaining double-stranded DNA derived from PII- or PI.3-specific aromatase mRNA was quantified using the same primer and probe set for the aromatase coding region–specific real-time PCR. Another aliquot of the purified DNA sample was directly subjected to

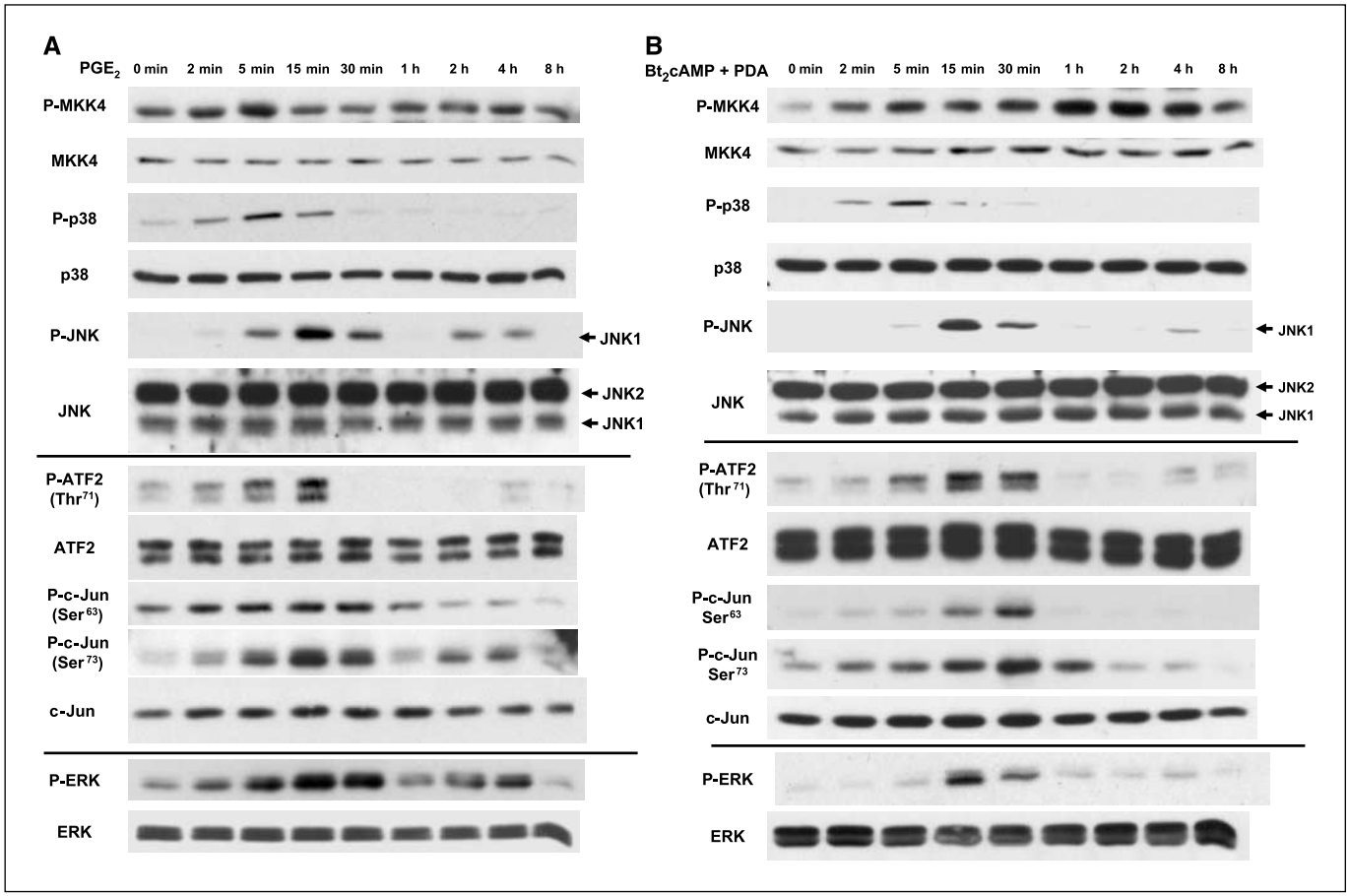

Figure 1. Treatment with PGE_2 or Bt_2cAMP + PDA stimulates the p38, JNK, and ERK MAPK pathways. BAFs were serum starved for 16 h and treated with 1 μmol/L PGE_2 (*A*) or 0.5 mmol/L Bt_2cAMP plus 100 nmol/L PDA (*B*) for the indicated times. Whole-cell lysates were prepared and subjected to SDS-PAGE and immunoblotting with the indicated antibodies.

the GAPDH real-time PCR protocol without *Exo*I treatment. The relative amounts of GAPDH reflected the relative amounts of the input single-stranded cDNA templates and were used to normalize the levels of promoter-specific aromatase mRNA. The amount of GAPDH in *Exo*I-treated samples was 0.5^{10} of that in nontreated counterparts, indicating complete removal of single-stranded cDNA with *Exo*I. For aromatase PI.4–derived mRNA real-time PCR, the forward and reverse primers were 5′-GTAGAACGTGACCAACTGGAG-3′ and 5′-AGGCACGATGCTGGTGATG-3′, and the fluorescence-labeled probe was 5′-ATGGGCTGACCAGTGCCAGG-GACC-3′.

Aromatase activity assay. The aromatase activity of BAFs was measured by the $[^3H]H_2O$ release assay as previously described (20). Of note, after BAFs were serum starved and treated as indicated in the figure legends, the mixture of $[^3H]$-labeled and cold androstenedione was added to the medium, and incubation was continued for another 6 h.

Small interfering RNA knockdown. BAFs were transfected with a nontargeting negative control small interfering RNA (siRNA; Dharmacon) or siRNAs against p38α (Dharmacon) and/or JNK1 (Invitrogen) at a final concentration of 100 nmol/L using Lipofectamine RNAiMAX (Invitrogen). Mock transfection was conducted with Lipofectamine RNAiMAX only. Seventy-two hours after transfection, cells were serum starved for 16 h, treated or not with 1 μmol/L PGE_2 for 6 h, and processed for immunoblotting, real-time PCR, and aromatase activity assays.

Chromatin immunoprecipitation. BAFs were grown in 15-cm dishes to confluence, serum starved for 16 h, and incubated in the presence or absence of 1 μmol/L PGE_2 or 0.5 mmol/L Bt_2cAMP plus 100 nmol/L PDA as indicated in the figure legends. The cells were harvested and subjected to chromatin immunoprecipitation with an anti–c-Jun antibody (Santa Cruz Biotechnology), an anti–phospho-ATF2 antibody (Santa Cruz Biotechnology), or a control rabbit immunoglobulin G (IgG; Santa Cruz Biotechnology) as described (20). The aromatase proximal primers have been described by Ghosh et al. (37): 5′-AACCTGCTGATGAAGTCACAA-3′ and 5′-TCAGACATT-TAGGCAAGACT-3′. The amplified DNA sequence encompassed the −302/−38 bp region of aromatase PI.3/PII.

Results

PGE_2 and Bt_2cAMP + PDA stimulate p38, JNK, and ERK MAPKs. In BAFs, PGE_2 is a potent stimulator of aromatase expression, and this effect is mimicked by Bt_2cAMP + PDA (6, 10, 14, 16, 17, 20). To identify the signaling events involved in PGE_2-induced aromatase expression, we examined phosphorylation of molecules within the p38, JNK, and ERK MAPK pathways. MKK4, a MAP2K within the p38 and JNK pathways, was rapidly phosphorylated following PGE_2 stimulation, reaching a peak by 5 min and declining to basal level by 30 min. MKK4 underwent a second phase of phosphorylation 1 to 4 h following PGE_2 treatment (Fig. 1*A, top*). Because MKK4 is an upstream activating kinase of p38 and JNK, phosphorylation of p38 and JNK1 was also induced rapidly by PGE_2 (refs. 22, 23; Fig. 1*A, top*). Remarkably, JNK1 and its substrate c-Jun (on Ser^{73}) exhibited a biphasic phosphorylation similar to that of MKK4 (Fig. 1 *A, top* and *middle*). Ser^{63} phosphorylation of c-Jun, by contrast, was largely unchanged during the first 30 min following PGE_2 stimulation

and declined over time (Fig. 1*A, middle*). ATF2 is an *in vivo* substrate of both p38 and JNK (19, 20, 38). As expected, PGE_2 induced acute phosphorylation of ATF2 (Fig. 1*A, middle*). The ERK1/2 MAPKs were also stimulated by PGE_2, exhibiting a biphasic phosphorylation very similar to that of JNK1 (Fig. 1*A, bottom*).

By simultaneously activating PKA and PKC signaling pathways, Bt_2cAMP + PDA mimics the action of PGE_2, including induction of

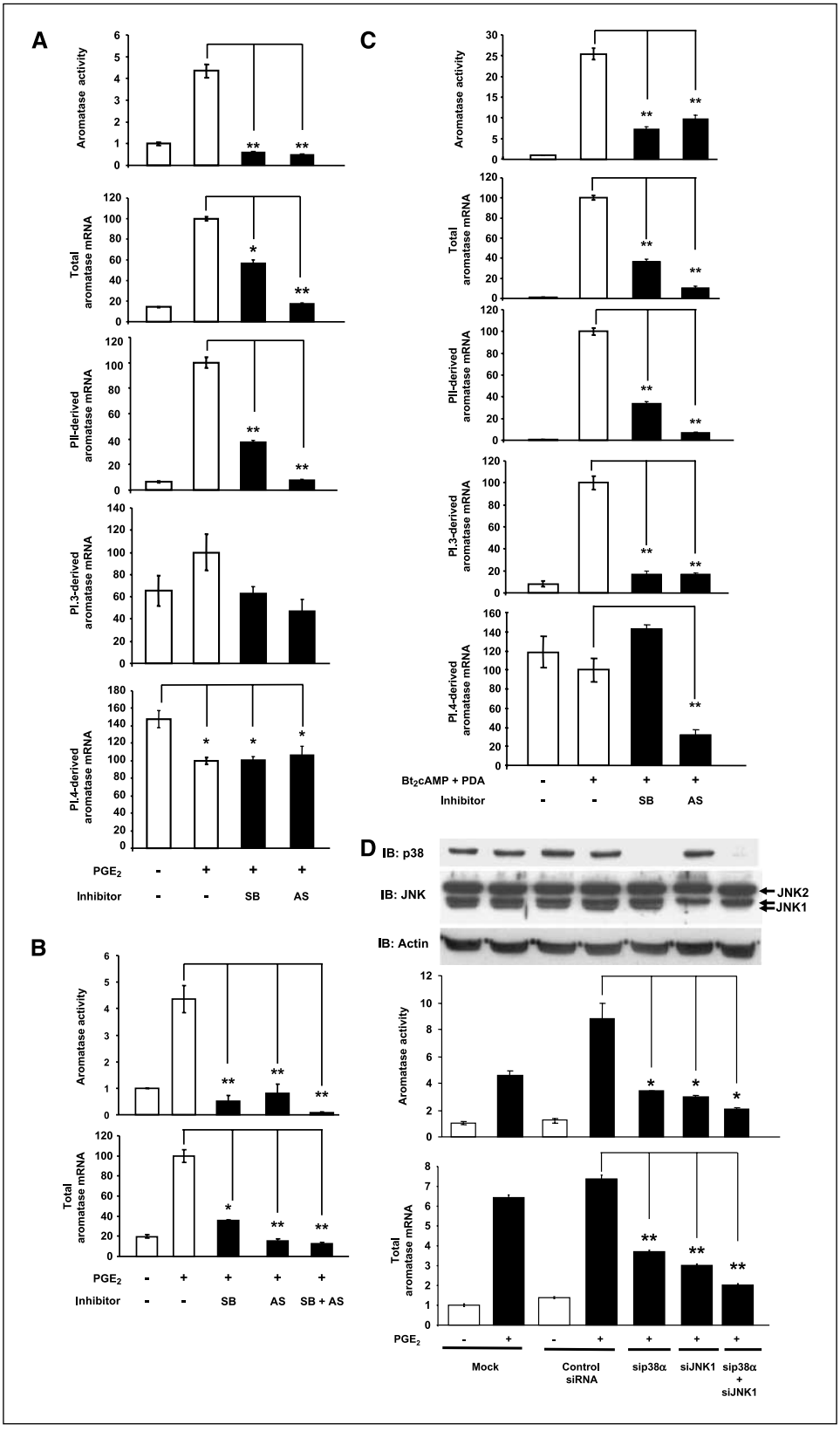

Figure 2. *A* to *C,* inhibition of p38 or JNK blocks PGE_2- or Bt_2cAMP + PDA–stimulated aromatase activity and induction of aromatase mRNA levels. Following a 16-h serum starvation, BAFs were pretreated with DMSO (−), 5 μmol/L SB202190 (*SB*), and/or 5 μmol/L AS601245 (*AS*) for 1 h. Cells were subsequently treated with 1 μmol/L PGE_2 for 6 h (*A* and *B*) or 0.5 mmol/L Bt_2cAMP plus 100 nmol/L PDA for 24 h (*C*). Aromatase activity assays and quantification of aromatase mRNA levels using TaqMan-based real-time PCR were done. Basal aromatase activity with DMSO pretreatment was normalized to 1. The levels of aromatase mRNA stimulated by PGE_2 or Bt_2cAMP + PDA in the presence of DMSO were taken as 100%. *D,* siRNA-mediated knockdown of p38α and/or JNK1 reduced PGE_2-stimulated aromatase activity and induction of aromatase mRNA levels. BAFs were mock-transfected or transfected with the indicated siRNAs, serum starved, and treated or not with 1 μmol/L PGE_2 for 6 h as described in Materials and Methods. Cells were then harvested for immunoblotting with anti-p38, anti-JNK, and anti-actin antibodies; aromatase coding region–specific real-time PCR; or subjected to aromatase activity assays as described in Materials and Methods. Basal aromatase activity and total aromatase mRNA level in mock-transfected BAFs were normalized to 1. *A* to *D, columns,* mean aromatase activities and aromatase mRNA levels from four independent measurements for each condition; *bars,* SE. *, $P < 0.05$; **, $P < 0.01$ (paired *t* test).

aromatase expression in BAFs (10, 14, 16, 17). Like PGE_2, Bt_2cAMP + PDA stimulated phosphorylation of MKK4, p38, JNK1, ATF2, c-Jun (on both Ser^{63} and Ser^{73}), and ERK1/2 (Fig. 1*B*); however, the biphasic pattern of MKK4, JNK1, c-Jun, and ERK phosphorylation was less prominent (Fig. 1*B*). Taken together, these data indicate that PGE_2 and its surrogate hormonal mixture Bt_2cAMP + PDA stimulate the p38, JNK, and ERK MAPK pathways in BAFs.

Inhibition or siRNA-mediated knockdown of p38 or JNK1 reduces PGE_2-stimulated aromatase activity and mRNA levels in BAFs. We determined whether p38 and JNK1 activation by PGE_2 was required for PGE_2-stimulated aromatase activity and expression in BAFs. Because peak induction of total aromatase mRNA was reached 6 to 10 h following PGE_2 treatment (data not shown), we measured aromatase activity and mRNA levels in the absence or presence of the p38 and/or JNK inhibitors (SB202190 and AS601245, respectively) following PGE_2 treatment for 6 h (39, 40). PGE_2 induced a 4- to 5-fold increase in aromatase activity, which was reduced to below basal levels in the presence of 5 μmol/L SB202190 or AS601245 (Fig. 2*A*).

Increased aromatase activity with PGE_2 treatment results from increased aromatase gene expression (10, 16, 41). Using real-time reverse transcription-PCR (RT-PCR), we found that PGE_2 treatment resulted in a 6- to 7-fold increase in total aromatase mRNA. Addition of either SB202190 or AS601245 markedly reduced this induction by ~40% and 80%, respectively (Fig. 2*A*). Basal levels of aromatase expression are maintained by a weak aromatase promoter, PI.4, whereas PGE_2-induced aromatase expression results from increased activity of aromatase PII and, to a lesser extent, PI.3 (10). Using aromatase promoter-specific real-time RT-PCRs, we quantified aromatase transcripts derived from these promoters. PGE_2 treatment led to a robust increase in PII-derived aromatase mRNA level, and it was significantly inhibited by SB202190 or AS601245 (Fig. 2*A*). Consistent with the previous report (10), PGE_2 induced a very weak and statistically insignificant increase in PI.3-derived aromatase mRNA level, and it was completely abolished by the p38 or JNK inhibitor (Fig. 2*A*). Unlike aromatase PII–derived mRNA, aromatase PI.4–derived mRNA was significantly down-regulated by 33% following a 6-h PGE_2 treatment, suggesting that aromatase PI.4 activity is subjected to reciprocal negative regulation. Neither the p38 nor the JNK inhibitor caused any further changes in PI.4-derived mRNA levels (Fig. 2*A*).

The effects of the p38 and JNK inhibitors were additive because dual blockade of p38 and JNK with both inhibitors completely ablated PGE_2 induction of aromatase, reducing its activity and total mRNA to sub-basal levels (Fig. 2*B*).

Unlike PGE_2, Bt_2cAMP + PDA induced a more persistent and sharper increase of total aromatase mRNA that started to plateau 24 h following the treatment (data not shown). Thus, we chose Bt_2cAMP + PDA treatment for 24 h, when total aromatase mRNA level was near its peak, to examine the effects of the p38 and JNK inhibitors on aromatase induction (Fig. 2*C*). Bt_2cAMP + PDA induced a 25-fold increase in aromatase activity, which was markedly reduced by SB202190 or AS601245. In parallel, Bt_2cAMP + PDA stimulated a nearly 100-fold increase in total aromatase mRNA. Likewise, the p38 or JNK inhibitor markedly diminished Bt_2cAMP + PDA–dependent induction of total aromatase mRNA and aromatase PII– and PI.3–derived mRNA levels. PI.4-generated aromatase mRNA tended to decrease following a 24-h Bt_2cAMP + PDA treatment; however, this was not statistically significant (Fig. 2*C*). Unlike SB202190, treatment with AS601245 for 24 h reduced PI.4-specific mRNA levels in the presence or absence of

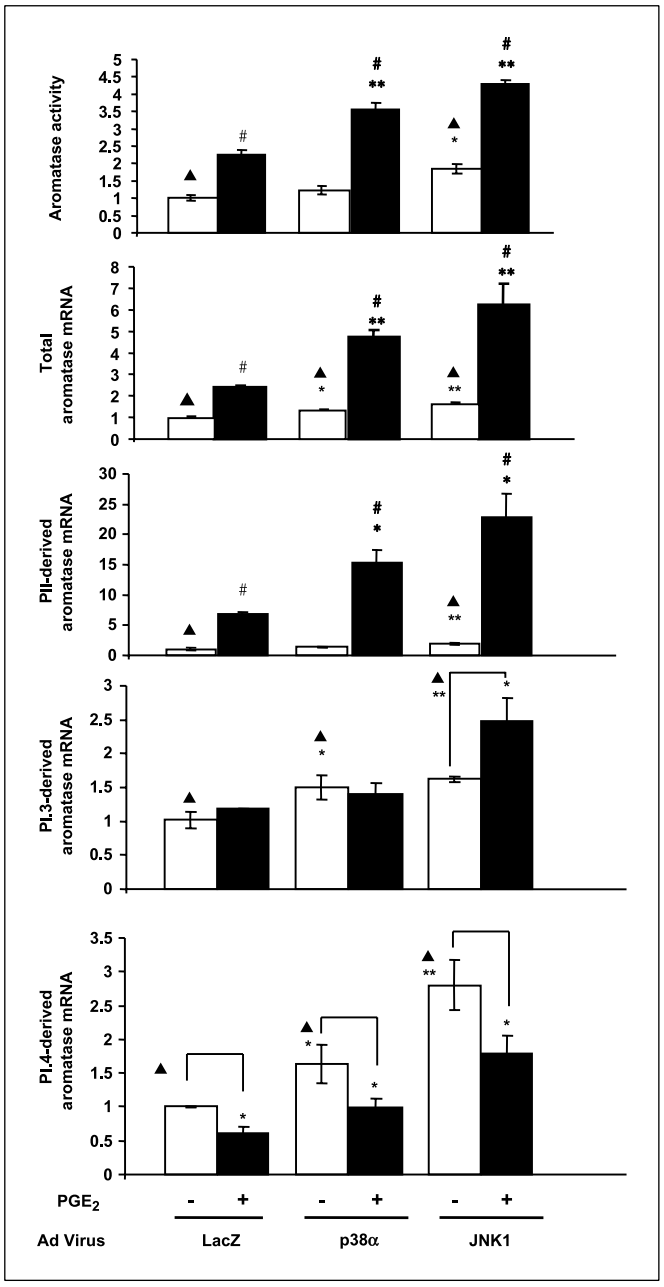

Figure 3. Overexpression of p38α or JNK1 promotes PGE_2 induction of aromatase activity and aromatase mRNA levels. BAFs were infected with a control adenovirus encoding LacZ, an adenovirus encoding p38α, or an adenovirus encoding JNK1 at an MOI of 20. Thirty-six hours later, the cells were serum starved for 16 h followed by treatment or not with 1 μmol/L PGE_2 for 6 h. Aromatase activity assays and aromatase coding region– and promoter-specific real-time RT-PCRs were done as described in Materials and Methods. Basal aromatase activity and levels of aromatase mRNA in LacZ-infected control cells were normalized to 1. *Columns,* mean aromatase activities and aromatase mRNA levels from four independent measurements for each condition; *bars,* SE. ▲ and #, pairwise comparisons of cells overexpressing p38α or JNK1 with control cells overexpressing LacZ in the basal and PGE_2-stimulated states, respectively. *, $P < 0.05$; **, $P < 0.01$ (paired *t* test).

Bt_2cAMP + PDA (Fig. 2*C*, and data not shown). PGE_2 or Bt_2cAMP + PDA also activated ERK (Fig. 1). When we used the MEK inhibitor PD98059 to block ERK phosphorylation/activation, we found that PGE_2- or Bt_2cAMP + PDA–induced total aromatase mRNA levels were not significantly altered (Supplementary Fig. S1*A* and *B*).

To validate the roles of p38 and JNK1 in PGE_2 regulation of aromatase, we used siRNAs to knock down p38α and/or JNK1 (Fig. 2*D*). In mock- or control siRNA–transfected BAFs, PGE_2 stimulated a marked increase in aromatase activity and total mRNA levels. BAFs transfected with sip38α had an undetectable p38 protein level and a significant reduction in PGE_2-induced aromatase activity and total aromatase mRNA level. Likewise, transfection of siJNK1, which abolished the expression of the shorter JNK1 splice variants α1/β1 and which decreased the level of the longer variants α2/β2, had a similar effect. Transfection of both sip38α and siJNK1 further suppressed PGE_2-stimulated aromatase activity and mRNA level.

Taken together, these results indicate that activation of p38 and JNK1, but not ERK, is necessary for PGE_2- or Bt_2cAMP + PDA–dependent induction of aromatase expression via activation of aromatase PI.3/PII. They also suggest that the JNK pathway plays a positive role in maintaining baseline PI.4 activity.

Overexpression of wild-type p38α or JNK1 enhances PGE_2 induction of aromatase mRNA levels. Conversely, we determined whether overexpression of p38α or JNK1 would enhance aromatase activity and promoter-specific aromatase expression. p38α is a ubiquitously expressed and SB inhibitor–sensitive isoform of p38 (25). We infected BAFs with either a control adenovirus encoding LacZ or an adenovirus encoding p38α or JNK1, followed by PGE_2 treatment (Fig. 3). Compared with that of LacZ, adenoviral overexpression of p38α or JNK1 markedly enhanced PGE_2 induction of aromatase activity, total aromatase mRNA, and PII-derived mRNA levels. Overexpression of p38α caused a weak, but significant, increase in basal total aromatase mRNA level (1.32 ± 0.05-fold over LacZ, $P < 0.05$), associated with significant increases in PI.3-derived (1.50 ± 0.17-fold over LacZ, $P < 0.05$) and PI.4-derived (1.64 ± 0.29-fold over LacZ, $P < 0.05$) aromatase mRNA. However, that was not sufficient to significantly increase basal aromatase activity. Overexpression of JNK1, by contrast, caused a significant increase in basal aromatase activity (1.85 ± 0.14-fold over LacZ, $P < 0.05$), associated with greater increases in basal total aromatase mRNA levels (1.61 ± 0.07-fold over LacZ, $P < 0.01$) derived from PI.3 (1.63 ± 0.04-fold over LacZ, $P < 0.01$), PII (1.91 ± 0.19-fold over LacZ, $P < 0.01$), and PI.4 (2.81 ± 0.37-fold over LacZ, $P < 0.01$). Similar to our earlier observations (Fig. 2*A*), PGE_2 treatment had little effect on PI.3-derived aromatase mRNA levels in LacZ- and p38α-expressing cells; however, it significantly stimulated PI.3 usage in JNK1-overexpressing cells. In addition, PI.4-derived mRNA levels were down-regulated to a similar extent (38% on average) in all overexpression groups following PGE_2 treatment (Fig. 3). Taken together, these data indicate that both p38α- and JNK1-dependent signaling pathways support PGE_2 activation of aromatase PII, and that the JNK1-dependent signaling pathway also greatly enhances the activity of aromatase PI.3 and PI.4.

PGE_2 or Bt_2cAMP + PDA stimulates binding of c-Jun and phosphorylated ATF2 to the aromatase promoter I.3/II region. The dependence of PGE_2- or Bt_2cAMP + PDA–induced aromatase expression on JNK and p38 suggested that their substrates c-Jun and/or ATF2 may regulate aromatase expression by interacting with aromatase PI.3/PII. To determine c-Jun binding to aromatase PI.3/PII, we treated BAFs with either PGE_2 for 15 min or Bt_2cAMP + PDA for 30 min, treatments which stimulated peak c-Jun phosphorylation (Fig. 1), and carried out chromatin immunoprecipitation assays with an anti–c-Jun antibody followed by aromatase PI.3/PII–specific PCR (Fig. 4*A*). In untreated cells, we did not detect significant c-Jun binding to aromatase PI.3/PII (Fig. 4*A*). Following PGE_2 or Bt_2cAMP + PDA treatment, there was a marked increase in c-Jun binding (Fig. 4*A*). Likewise, we carried out chromatin immunoprecipitation with a phospho-specific ATF2 antibody, and found that treatment with PGE_2 for 15 min, which stimulated peak ATF2 phosphorylation (Fig. 1), resulted in binding of phosphorylated ATF2 to aromatase PI.3/PII (Fig. 4*B*). Taken together, these data suggest that PGE_2 or Bt_2cAMP + PDA enhances c-Jun and ATF2 binding to aromatase PI.3/PII, thus allowing c-Jun and ATF2 to stimulate aromatase gene transcription.

cAMP- and PKC-dependent pathways contribute to p38 and JNK activation. To determine the cAMP effector(s) responsible for p38 and JNK activation and induction of aromatase in BAFs, we used a PKA-specific cAMP analogue (6-MB-cAMP) or an EPAC-specific cAMP analogue (8-pCPT-2′-*O*-Me-cAMP), along with Bt_2cAMP that activates both PKA and EPAC (42, 43). All three cAMP analogues induced p38, JNK1, and ERK phosphorylation (Fig. 5*A*). In contrast, only the PKA-activating cAMP analogues, 6-MB-cAMP and Bt_2cAMP, strikingly induced aromatase mRNA levels, whereas the EPAC-specific analogue 8-pCPT-2′-*O*-Me-cAMP did not (Fig. 5*B*). These data indicate that both PKA and EPAC mediate cAMP-stimulated p38 and JNK activation, whereas activation of PKA, but not EPAC, is responsible for aromatase induction. Moreover, activation of p38 and JNK seems to be required, but not sufficient, for aromatase induction.

We further examined the relative roles of cAMP and PDA/PKC in stimulation of p38 and JNK1, and induction of aromatase mRNA levels. Compared with Bt_2cAMP, PDA induced comparable p38 phosphorylation and greater JNK1 phosphorylation with a similar time course (Fig. 5*C*). However, PDA was a weaker stimulator of aromatase expression than Bt_2cAMP (Fig. 5*D*), although it synergistically enhanced Bt_2cAMP-stimulated aromatase gene transcription by ~9-fold (Fig. 5*D*). These data suggest that PKC

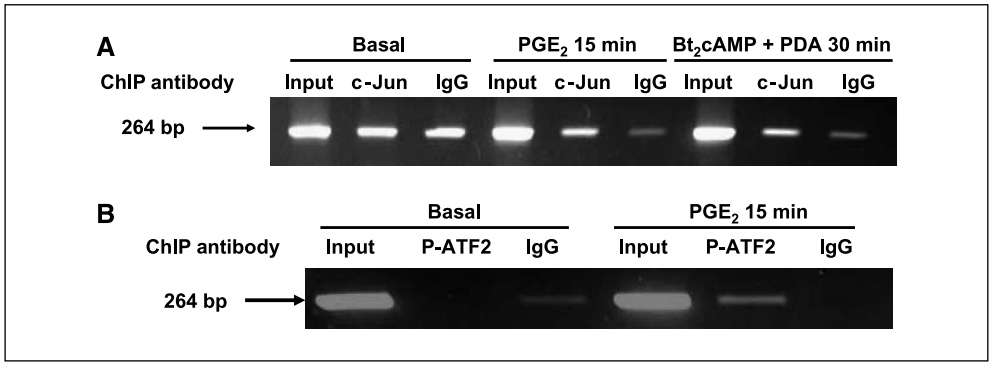

Figure 4. PGE_2 stimulates c-Jun and ATF2 binding to the aromatase PI.3/PII region. *A,* after a 16-h serum starvation, BAFs were treated with 1 μmol/L PGE_2 for 15 min or 0.5 mmol/L Bt_2cAMP plus 100 nmol/L PDA for 30 min. Cells were harvested and subjected to chromatin immunoprecipitation (*ChIP*) with an anti–c-Jun antibody or a control IgG. *B,* BAFs were serum starved for 16 h, after which they were treated with 1 μmol/L PGE_2 for 15 min. Cells were harvested and subjected to chromatin immunoprecipitation with a phospho-ATF2 antibody and a control IgG.

contributes to PGE_2- or Bt_2cAMP + PDA–stimulated p38 and JNK1 phosphorylation. They also indicate that activation of p38 and JNK1 by PDA without concurrent PKA activation is not sufficient for maximal aromatase induction.

Discussion

Our findings indicated that PGE_2 stimulated p38, JNK1, and ERK via cAMP and PKC. Among these, p38 and JNK1 were essential, but not sufficient, for PGE_2-dependent induction of aromatase expression mainly via PII. Interestingly, PGE_2-stimulated phosphorylation of MKK4, JNK1, c-Jun, and ERK exhibited a distinct biphasic pattern. This may reflect a cross talk among the EP receptors, kinases, and phosphatases involved in regulating the MAPK pathways. Indeed, when cells were treated with Bt_2cAMP + PDA, which bypasses EP receptor activation, biphasic phosphorylation was much less prominent. Richards et al. (14) showed that EP_3 also mediates PGE_2 action in BAFs by inhibiting the adenylate cyclase-PKA pathway and antagonizing signaling through EP_2. The dynamic net effect of EP receptor stimulation on the adenylate cyclase-cAMP-PKA pathway would determine activation or inactivation of downstream MAPK cascades.

Both PKA and EPACs mediate cAMP signaling (26). Although our findings suggest that PKA, but not EPAC, mediated the stimulatory effects of PGE_2 or cAMP on aromatase expression, we showed that EPACs as well as PKA were capable of stimulating p38, JNK1, and ERK phosphorylation, consistent with other published reports

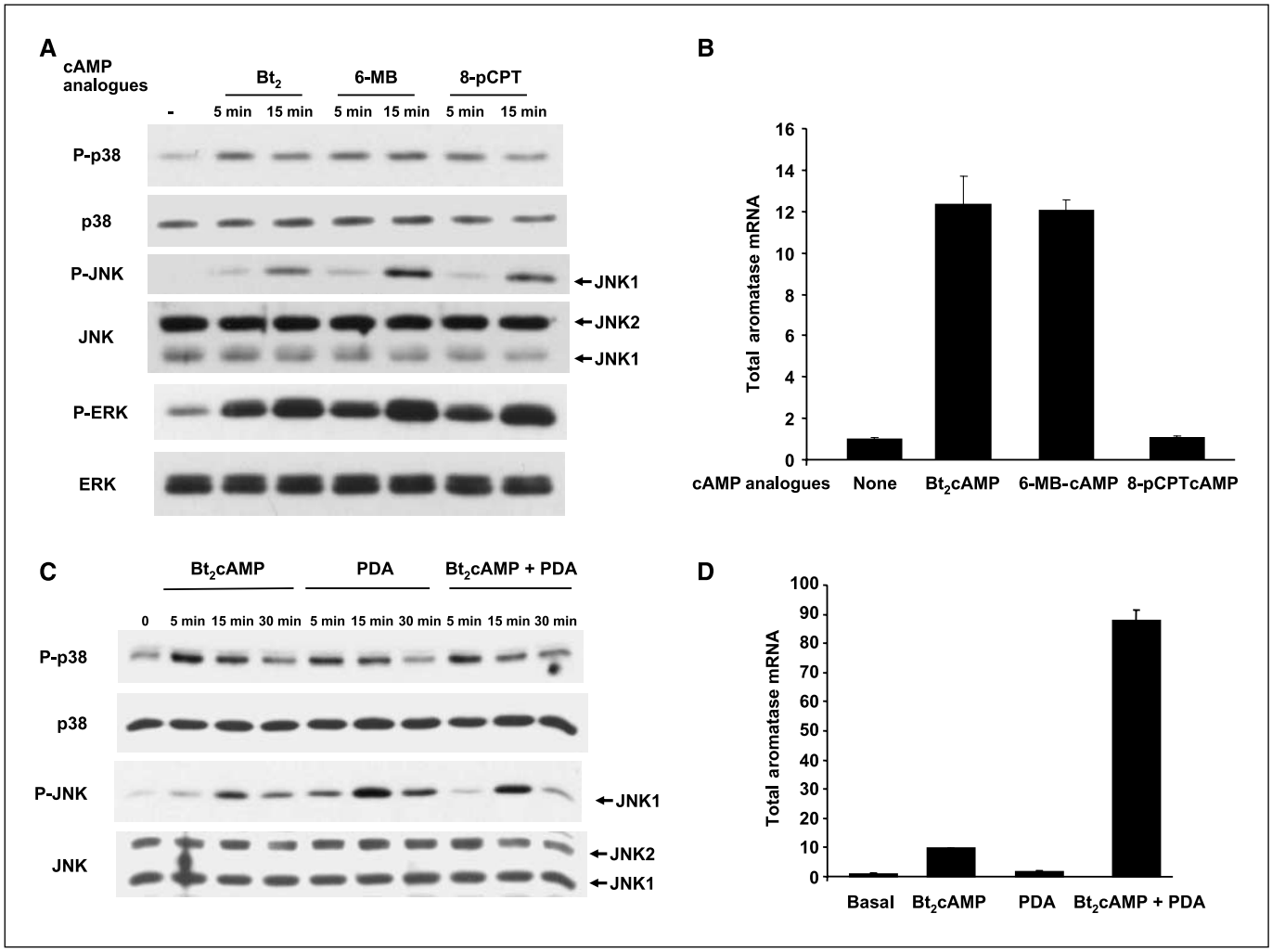

Figure 5. PKA, EPAC, and PKC mediate activation of p38 and JNK1. *A,* both effectors of cAMP mediate activation of p38, JNK1, and ERK MAPKs. BAFs were serum starved for 16 h. They were then either left untreated or stimulated with 50 μmol/L Bt_2cAMP (*Bt_2*; nonselective), 50 μmol/L 6-MB-cAMP (*6-MB*; PKA-specific), or 50 μmol/L 8-pCPT-2′-*O*-Me-cAMP (*8-pCPT*; EPAC-specific) for the indicated times. Whole-cell lysates were prepared and subjected to SDS-PAGE and immunoblotting with the indicated antibodies. *B,* cAMP induction of aromatase mRNA depends on PKA but not EPAC. BAFs were serum starved for 16 h. Cells were then either left untreated (*None*) or treated with 0.5 mmol/L Bt_2cAMP, 0.5 mmol/L 6-MB-cAMP, or 0.5 mmol/L 8-pCPT-2′-*O*-Me-cAMP (*8-pCPTcAMP*) for 24 h. Total RNA was isolated and subjected to aromatase coding region–specific real-time RT-PCR. The level of aromatase mRNA in the untreated cells was normalized to 1. *Columns,* mean of four independent measurements for each condition; *bars,* SE. *C,* Bt_2cAMP or PDA induces phosphorylation of p38 and JNK1. BAFs were serum starved for 16 h and were either untreated or treated with 0.5 mmol/L Bt_2cAMP alone, 100 nmol/L PDA alone, or 0.5 mmol/L Bt_2cAMP plus 100 nmol/L PDA for the indicated times. Cell lysates were prepared and subjected to SDS-PAGE and immunoblotting with the indicated antibodies. *D,* PDA activation of p38 and JNK1 is not sufficient for maximal induction of aromatase mRNA. BAFs were serum starved for 16 h and were either untreated (*Basal*) or treated with 0.5 mmol/L Bt_2cAMP alone, 100 nmol/L PDA alone, or 0.5 mmol/L Bt_2cAMP plus 100 nmol/L PDA for 24 h. Total RNA was isolated and subjected to aromatase coding region–specific real-time PCR. The level of aromatase mRNA in the untreated cells was normalized to 1. *Columns,* mean of four independent measurements for each condition; *bars,* SE.

indicating the roles of both PKA and EPACs in MAPK activation (28, 30–34, 44).

Our results were also consistent with published data about phorbol ester/PKC–dependent activation of p38 and JNK, which seems to involve PKC activation of the Ras-MEK kinase 1-MKK4 pathway (24, 25), and RACK1-facilitated PKC phosphorylation of JNK (35).

The p38 and JNK inhibitors had different efficacies particularly on PI.3 activities induced by PGE_2-and Bt_2cAMP + PDA, respectively. Bt_2cAMP + PDA was a more potent stimulator of aromatase than PGE_2 because it induces stronger aromatase activity, higher levels of total aromatase mRNA, and especially more robust PI.3 activity as well as that of PII. PGE_2, by contrast, led to a weak and statistically insignificant increase in PI.3 activity. Aromatase PI.3 contains an upstream activator protein-1 (AP-1) site and two cAMP-responsive element (CRE) sites (45). Similarly, aromatase PII contains a CRE site in the −211/−199 region (20). ATF2 can form homodimers or heterodimers with members of the ATF and AP-1 families, including c-Jun, and may regulate aromatase PI.3/PII via these CRE and/or AP-1 sites (46). Our chromatin immunoprecipitation assays showing binding of c-Jun and ATF2 to aromatase PI.3/PII support this idea. Thus, differential activation of ATF2 and c-Jun, which is indicative of activation of upstream p38 and JNK1, may account for differential activation of PI.3/PII. Indeed, Bt_2cAMP + PDA–induced peak ATF2 phosphorylation was more persistent (for up to 30 min), and c-Jun phosphorylation more robust (on both Ser^{63} and Ser^{73}), whereas PGE_2-stimulated ATF2 phosphorylation was shorter (for up to 15 min), and c-Jun phosphorylation weaker (only on Ser^{73}). Because relatively weak PGE_2 stimulation of both p38 and JNK1 barely stimulated PI.3, inhibiting one of the kinases readily returned PI.3 activity to the basal level (Fig. 2*A*). In contrast, because Bt_2cAMP + PDA stimulation of p38 and JNK1 was relatively strong, even complete inhibition of one kinase may still allow enough activity of the other to keep PI.3 usage a bit above the basal level as seen in Fig. 2*C*.

Using inhibitors, siRNA knockdown, and overexpression, we established the roles of p38α and JNK1 in PGE_2 regulation of aromatase expression. Furthermore, our data suggest that JNK1 is relatively more important than p38 for this regulation because, in blocking PGE_2 induction of aromatase mRNA levels, JNK inhibitor was more effective than the p38 inhibitor, and partial JNK1 knockdown was as effective as complete p38 knockdown; also, JNK1 overexpression had stronger and broader stimulatory effects on aromatase promoter activities. This is consistent with our hypothesis that p38 regulates aromatase expression through ATF2, and JNK regulates aromatase expression through both ATF2 and c-Jun. We previously showed binding of phosphorylated ATF2 to aromatase PI.3/PII in BAFs following treatment with MCF-7 cell-conditioned medium (20). Here, we showed that PGE_2 stimulated binding of c-Jun and ATF2 to aromatase PI.3/PII and that the binding coincided with peak phosphorylation and, therefore, peak transactivational activity of the proteins. Ghosh et al. (37) have identified the CRE element of aromatase PII as the c-Jun binding site in granulosa cells; however, c-Jun represses rather than promotes aromatase expression in those cells. Our preliminary results suggested that ATF2 and c-Jun bound to the same element in BAFs (data not shown). Because ATF2 and c-Jun are broad regulators of gene expression, we cannot rule out the possibility that p38 or JNK stimulates aromatase expression indirectly.

Given the presence of an upstream AP-1 site in PI.4 that ATF2 and c-Jun may jointly regulate (47), it is not surprising that

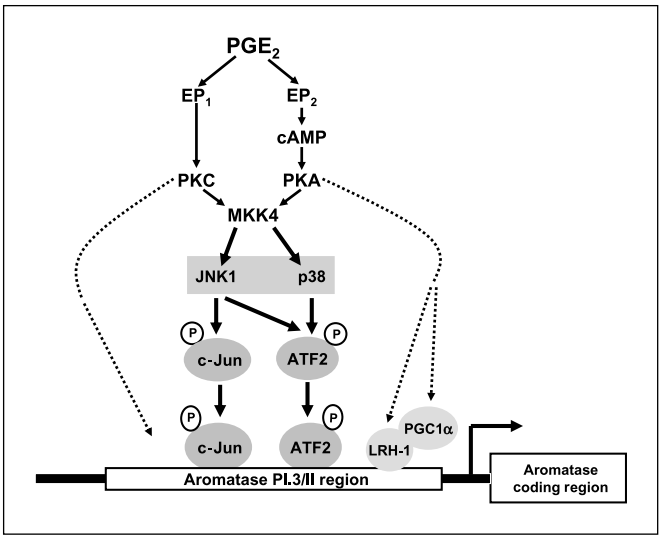

Figure 6. Model of PGE_2 regulation of aromatase expression via PI.3/PII. PGE_2 binds to the EP_1 and EP_2 receptors and stimulates the PKC and adenylate cyclase-cAMP-PKA pathways, respectively. Both PKA and PKC contribute to activation of MKK4, JNK1, and p38, resulting in phosphorylation and activation of transcription factors c-Jun and ATF2. Active c-Jun and ATF2 bind to the aromatase PI.3/PII region and promote aromatase gene transcription. Activation of the p38 and JNK pathways is necessary, but not sufficient, for maximal PGE_2 induction of aromatase, which requires collaboration among various signaling pathways downstream of PKA and PKC, and concerted up-regulation and/or activation of a number of transcription factors and coactivators such as c-Jun, ATF2, LRH-1, and PGC1α.

overexpression of p38α or JNK1 increased baseline PI.4-specific aromatase mRNA level, and that the JNK inhibitor AS601245 markedly reduced it during a 24-h period. Indeed, Zhao et al. (47) have observed that c-Jun and the p38-dependent pathway were important for PI.4 activation.

Other transcriptional enhancers that regulate aromatase gene expression in BAFs have been identified, including PGC1α and LRH-1 (48–50). LRH-1 binds to a nuclear receptor half site within aromatase PI.3/PII and promotes aromatase expression (49). By associating with LRH-1, PGC1α is a coactivator and enhances the transcriptional activity of LRH-1 (50). In BAFs, PKA stimulates PGC1α expression, and both PKA and PKC stimulate the expression of LRH-1 (48, 50).

We found that EPAC or PDA activation of p38 and JNK1 without PKA stimulation was not sufficient for appreciable induction of aromatase expression in BAFs. We hypothesize that maximal PGE_2 or Bt_2cAMP + PDA induction of aromatase expression entails collaboration among various signaling pathways downstream of PKA and PKC, resulting in concerted up-regulation and/or activation of a number of transcription factors, including c-Jun, ATF2, LRH-1, and PGC1α (Fig. 6). Further studies are needed to elucidate the signaling pathways and downstream transcription factors that transactivate the aromatase promoter region, and to identify additional potential molecular targets for breast cancer–selective inhibition of aromatase expression.

Acknowledgments

Received 1/8/2007; revised 6/6/2007; accepted 7/9/2007.

Grant support: NIH grant CA67167 and funds from the AVON Foundation, the Northwestern Memorial Foundation, and the Lynn Sage Cancer Research Foundation.

The costs of publication of this article were defrayed in part by the payment of page charges. This article must therefore be hereby marked *advertisement* in accordance with 18 U.S.C. Section 1734 solely to indicate this fact.

References

1. Bulun SE, Lin Z, Imir G, et al. Regulation of aromatase expression in estrogen-responsive breast and uterine disease: from bench to treatment. Pharmacol Rev 2005; 57:359–83.
2. O'Neill JS, Elton RA, Miller WR. Aromatase activity in adipose tissue from breast quadrants: a link with tumour site. Br Med J (Clin Res Ed) 1988;296:741–3.
3. Bulun SE, Price TM, Aitken J, Mahendroo MS, Simpson ER. A link between breast cancer and local estrogen biosynthesis suggested by quantification of breast adipose tissue aromatase cytochrome *P*450 transcripts using competitive polymerase chain reaction after reverse transcription. J Clin Endocrinol Metab 1993;77:1622–8.
4. Meng L, Zhou J, Sasano H, et al. Tumor necrosis factor α and interleukin 11 secreted by malignant breast epithelial cells inhibit adipocyte differentiation by selectively down-regulating CCAAT/enhancer binding protein α and peroxisome proliferator-activated receptor γ: mechanism of desmoplastic reaction. Cancer Res 2001;61:2250–5.
5. Bulun SE, Takayama K, Suzuki T, et al. Organization of the human aromatase p450 (CYP19) gene. Semin Reprod Med 2004;22:5–9.
6. Mahendroo MS, Mendelson CR, Simpson ER. Tissue-specific and hormonally controlled alternative promoters regulate aromatase cytochrome *P*450 gene expression in human adipose tissue. J Biol Chem 1993; 268:19463–70.
7. Zhao Y, Mendelson CR, Simpson ER. Characterization of the sequences of the human CYP19 (aromatase) gene that mediate regulation by glucocorticoids in adipose stromal cells and fetal hepatocytes. Mol Endocrinol 1995;9:340–9.
8. Baum M, Budzar AU, Cuzick J, et al. Anastrozole alone or in combination with tamoxifen versus tamoxifen alone for adjuvant treatment of postmenopausal women with early breast cancer: first results of the ATAC randomised trial. Lancet 2002;359:2131–9.
9. Morales L, Neven P, Paridaens R. Choosing between an aromatase inhibitor and tamoxifen in the adjuvant setting. Curr Opin Oncol 2005;17:559–65.
10. Zhao Y, Agarwal VR, Mendelson CR, Simpson ER. Estrogen biosynthesis proximal to a breast tumor is stimulated by PGE2 via cyclic AMP, leading to activation of promoter II of the CYP19 (aromatase) gene. Endocrinology 1996;137:5739–42.
11. Purohit A, Ghilchik MW, Duncan L, et al. Aromatase activity and interleukin-6 production by normal and malignant breast tissues. J Clin Endocrinol Metab 1995; 80:3052–8.
12. Schrey MP, Patel KV. Prostaglandin E2 production and metabolism in human breast cancer cells and breast fibroblasts. Regulation by inflammatory mediators. Br J Cancer 1995;72:1412–9.
13. Diaz-Cruz ES, Shapiro CL, Brueggemeier RW. Cyclooxygenase inhibitors suppress aromatase expression and activity in breast cancer cells. J Clin Endocrinol Metab 2005;90:2563–70.
14. Richards JA, Brueggemeier RW. Prostaglandin E2 regulates aromatase activity and expression in human adipose stromal cells via two distinct receptor subtypes. J Clin Endocrinol Metab 2003;88:2810–6.
15. Breyer RM, Bagdassarian CK, Myers SA, Breyer MD. Prostanoid receptors: subtypes and signaling. Annu Rev Pharmacol Toxicol 2001;41:661–90.
16. Mendelson CR, Corbin CJ, Smith ME, Smith J, Simpson ER. Growth factors suppress and phorbol esters potentiate the action of dibutyryl adenosine 3′,5′-monophosphate to stimulate aromatase activity of human adipose stromal cells. Endocrinology 1986;118: 968–73.
17. Evans CT, Corbin CJ, Saunders CT, et al. Regulation of estrogen biosynthesis in human adipose stromal cells. Effects of dibutyryl cyclic AMP, epidermal growth factor, and phorbol esters on the synthesis of aromatase cytochrome P-450. J Biol Chem 1987;262:6914–20.
18. Yu FQ, Han CS, Yang W, et al. Activation of the p38 MAPK pathway by follicle-stimulating hormone regulates steroidogenesis in granulosa cells differentially. J Endocrinol 2005;186:85–96.
19. Raingeaud J, Whitmarsh AJ, Barrett T, Derijard B, Davis RJ. MKK3- and MKK6-regulated gene expression is mediated by the p38 mitogen-activated protein kinase signal transduction pathway. Mol Cell Biol 1996;16: 1247–55.
20. Deb S, Zhou J, Amin SA, et al. A novel role of sodium butyrate in the regulation of cancer-associated aromatase promoters I.3 and II by disrupting a transcriptional complex in breast adipose fibroblasts. J Biol Chem 2006; 281:2585–97.
21. Schonwasser DC, Marais RM, Marshall CJ, Parker PJ. Activation of the mitogen-activated protein kinase/extracellular signal-regulated kinase pathway by conventional, novel, and atypical protein kinase C isotypes. Mol Cell Biol 1998;18:790–8.
22. Davis RJ. Signal transduction by the JNK group of MAP kinases. Cell 2000;103:239–52.
23. Roux PP, Blenis J. ERK and p38 MAPK-activated protein kinases: a family of protein kinases with diverse biological functions. Microbiol Mol Biol Rev 2004;68: 320–44.
24. Rebollo A, Martinez AC. Ras proteins: recent advances and new functions. Blood 1999;94:2971–80.
25. Kyriakis JM, Avruch J. Mammalian mitogen-activated protein kinase signal transduction pathways activated by stress and inflammation. Physiol Rev 2001;81:807–69.
26. Bos JL. Epac: a new cAMP target and new avenues in cAMP research. Nat Rev Mol Cell Biol 2003;4:733–8.
27. Hess A, Wijayanti N, Neuschafer-Rube AP, et al. Phorbol ester-dependent activation of peroxiredoxin I gene expression via a protein kinase C, Ras, p38 mitogen-activated protein kinase signaling pathway. J Biol Chem 2003;278:45419–34.
28. Gerlo S, Verdood P, Hooghe-Peters EL, Kooijman R. Multiple, PKA-dependent and PKA-independent, signals are involved in cAMP-induced PRL expression in the eosinophilic cell line Eol-1. Cell Signal 2005;17:901–9.
29. Maizels ET, Cottom J, Jones JC, Hunzicker-Dunn M. Follicle stimulating hormone (FSH) activates the p38 mitogen-activated protein kinase pathway, inducing small heat shock protein phosphorylation and cell rounding in immature rat ovarian granulosa cells. Endocrinology 1998;139:3353–6.
30. Wang Z, Dillon TJ, Pokala V, et al. Rap1-mediated activation of extracellular signal-regulated kinases by cyclic AMP is dependent on the mode of Rap1 activation. Mol Cell Biol 2006;26:2130–45.
31. Zhang B, Perpetua M, Fulmer M, Harbrecht BG. JNK signaling involved in the effects of cyclic AMP on IL-1β plus IFNγ-induced inducible nitric oxide synthase expression in hepatocytes. Cell Signal 2004;16:837–46.
32. Shi GX, Rehmann H, Andres DA. A novel cyclic AMP-dependent Epac-Rit signaling pathway contributes to PACAP38-mediated neuronal differentiation. Mol Cell Biol 2006;26:9136–47.
33. Hochbaum D, Tanos T, Ribeiro-Neto F, Altschuler D, Coso OA. Activation of JNK by Epac is independent of its activity as a Rap guanine nucleotide exchanger. J Biol Chem 2003;278:33738–46.
34. Laroche-Joubert N, Marsy S, Michelet S, Imbert-Teboul M, Doucet A. Protein kinase A-independent activation of ERK and H,K-ATPase by cAMP in native kidney cells: role of Epac I. J Biol Chem 2002;277: 18598–604.
35. Lopez-Bergami P, Habelhah H, Bhoumik A, et al. RACK1 mediates activation of JNK by protein kinase C [corrected]. Mol Cell 2005;19:309–20.
36. Chen D, Fucini RV, Olson AL, Hemmings BA, Pessin JE. Osmotic shock inhibits insulin signaling by maintaining Akt/protein kinase B in an inactive dephosphorylated state. Mol Cell Biol 1999;19:4684–94.
37. Ghosh S, Wu Y, Li R, Hu Y. Jun proteins modulate the ovary-specific promoter of aromatase gene in ovarian granulosa cells via a cAMP-responsive element. Oncogene 2005;24:2236–46.
38. Gupta S, Campbell D, Derijard B, Davis RJ. Transcription factor ATF2 regulation by the JNK signal transduction pathway. Science 1995;267:389–93.
39. Davies SP, Reddy H, Caivano M, Cohen P. Specificity and mechanism of action of some commonly used protein kinase inhibitors. Biochem J 2000;351:95–105.
40. Ferrandi C, Ballerio R, Gaillard P, et al. Inhibition of c-Jun N-terminal kinase decreases cardiomyocyte apoptosis and infarct size after myocardial ischemia and reperfusion in anaesthetized rats. Br J Pharmacol 2004; 142:953–60.
41. Agarwal VR, Bulun SE, Leitch M, Rohrich R, Simpson ER. Use of alternative promoters to express the aromatase cytochrome *P*450 (CYP19) gene in breast adipose tissues of cancer-free and breast cancer patients. J Clin Endocrinol Metab 1996;81:3843–9.
42. Mei FC, Qiao J, Tsygankova OM, et al. Differential signaling of cyclic AMP: opposing effects of exchange protein directly activated by cyclic AMP and cAMP-dependent protein kinase on protein kinase B activation. J Biol Chem 2002;277:11497–504.
43. Honegger KJ, Capuano P, Winter C, et al. Regulation of sodium-proton exchanger isoform 3 (NHE3) by PKA and exchange protein directly activated by cAMP (EPAC). Proc Natl Acad Sci U S A 2006;103:803–8.
44. Cao W, Daniel KW, Robidoux J, et al. p38 mitogen-activated protein kinase is the central regulator of cyclic AMP-dependent transcription of the brown fat uncoupling protein 1 gene. Mol Cell Biol 2004;24:3057–67.
45. Zhou D, Zhou C, Chen S. Gene regulation studies of aromatase expression in breast cancer and adipose stromal cells. J Steroid Biochem Mol Biol 1997;61: 273–80.
46. Hai T, Curran T. Cross-family dimerization of transcription factors Fos/Jun and ATF/CREB alters DNA binding specificity. Proc Natl Acad Sci U S A 1991; 88:3720–4.
47. Zhao Y, Nichols JE, Valdez R, Mendelson CR, Simpson ER. Tumor necrosis factor-α stimulates aromatase gene expression in human adipose stromal cells through use of an activating protein-1 binding site upstream of promoter 1.4. Mol Endocrinol 1996;10:1350–7.
48. Zhou J, Suzuki T, Kovacic A, et al. Interactions between prostaglandin E(2), liver receptor homologue-1, and aromatase in breast cancer. Cancer Res 2005;65: 657–63.
49. Clyne CD, Speed CJ, Zhou J, Simpson ER. Liver receptor homologue-1 (LRH-1) regulates expression of aromatase in preadipocytes. J Biol Chem 2002;277: 20591–7.
50. Safi R, Kovacic A, Gaillard S, et al. Coactivation of liver receptor homologue-1 by peroxisome proliferator-activated receptor γ coactivator-1α on aromatase promoter II and its inhibition by activated retinoid X receptor suggest a novel target for breast-specific antiestrogen therapy. Cancer Res 2005;65:11762–70.